Pre-scission neutron multiplicity in the $^{32}S + ^{184}W$ reaction

Prashant N. Patil,[1,*] N. M. Badiger,[1] B. K. Nayak,[2,3] S. Santra,[2,3] P. C. Rout,[2,3] A. Pal,[2] G. Mohanto,[2] K. Mahata,[2,3] K. Ramachandran,[2] R. G. Thomas,[2,3] E. T. Mirgule,[2] N. Madhavan,[4] Ramandeep Gandhi,[2] M. M. Hosamani,[1] A. Vinayak,[1] A. Kundu,[2] Sukanya De,[2,3] S. P. Behera,[2] B. Srinivasan,[2] A. Saxena,[2] and V. D. Bharud[5,6]

[1]*Department of Studies in Physics, Karnatak University, Dharwad 580003, India*
[2]*Nuclear Physics Division, Bhabha Atomic Research Centre, Mumbai 400085, India*
[3]*Homi Bhabha National Institute, Anushaktinagar, Mumbai 400094, India*
[4]*Inter University Accelerator Centre, Aruna Asaf Ali Marg, New Delhi 110067, India*
[5]*Department of Physics, Savitribai Phule Pune University, Pune 411007, India*
[6]*Department of Physics, M. J. College, Jalgaon 425002, India*

(Received 7 July 2020; accepted 2 September 2020; published 29 September 2020)

The neutron energy spectra in coincidence with both the correlated fission fragments in $^{32}S + ^{184}W$ reaction forming the compound nucleus ^{216}Th at an excitation energy of 71.31 MeV have been measured at various angles with respect to one of the fission fragments. Pre- and post-scission neutron multiplicities of 2.68 ± 0.48 and 3.3 ± 0.20, respectively, have been extracted by analyzing angular correlation of the neutron energy spectra using moving source fitting procedure. The excess pre-scission neutron multiplicity in comparison to statistical model JOANNE2 code predictions have been converted into total fission delay. A comparative study of fission delay has been carried out for the $^{16}O + ^{208}Pb$ reaction forming the compound nucleus ^{224}Th at similar excitation energy as in $^{32}S + ^{184}W$ reaction. Both the reactions have been analyzed within the frame work of JOANNE2 code including fission delay, deformation dependent level densities, particle binding energies, and transmission coefficients. The observed fission delay for both the reactions can be quantitatively understood if different formation time predicted by dynamical model HICOL code are considered.

DOI: 10.1103/PhysRevC.102.034618

I. INTRODUCTION

Heavy-ion-induced fusion-fission (HIFF) dynamics is an area of current research due to prominent signatures of entrance channel effects in fission-fragment mass distributions and particle multiplicities. A variety of experiments have been carried out in the past to explore the shell and dissipative effects in the HIFF process with various possible projectile and target combinations around the Coulomb barrier [1–8]. One of the major puzzles of HIFF reactions is the fission hindrance. The fission hindrance can be understood in terms of dissipation and fission delay time, which are responsible for the increased survival probability of the compound nucleus (CN), which in turn increases the emission of light charged particles, γ rays and neutrons from the excited CN. Extensive studies have been carried out in the past to estimate the fission delay time from pre-scission neutron, proton, α, and giant dipole resonance γ rays measurements in HIFF reactions [9–16]. The measured pre-scission neutron multiplicities were observed to be higher as compared to the statistical model predictions indicating the dynamical effect of nuclear fission. The cause for the excess emission of pre-scission neutrons arising from three distinct origins in FF dynamics can be qualitatively understood as follows. First, due to nuclear deexcitation an excess number of neutrons will be emitted from temperature equilibrated intermediate dinuclear system during its evolution towards the formation of CN, which is termed as formation delay (τ_{fr}). Second, as reported by Kramer [17] dissipation will delay the onset of fission event due to the occurrence of finite transition time as the equilibrium configuration diffuses over the saddle point causing an excess emission of neutrons. This delay is termed as transient delay (τ_{tr}). Third, in the postsaddle phase, dissipation causes excess emission of neutrons during the dynamical evolution of the system from saddle point to scission point (τ_{ssc}).

Since the last decade extensive measurements on neutrons in coincidence with fission fragments have been carried out for various entrance channel mass asymmetries at different excitation energies to provide an adequate explanation for excess emission of pre-scission neutrons during the presaddle to postsaddle region [1–5,11]. Wei has reported lower pre-scission neutron multiplicity (ν_{pre}) for shell-closed ($N = 126$) ^{216}Th nucleus compared to non-shell-closed ^{214}Th nucleus [10]. Sandal *et al.* [11] have measured the ν_{pre} for the compound nuclei $^{210,212,214,216}Rn$ formed in the reactions $^{16,18}O + ^{194,198}Pt$ in the excitation energy (E^*) range of 50–79 MeV and reported lower dissipation (β) for shell-closed ^{212}Rn isotope at the lowest $E^* = 50$ MeV.

In earlier works, fission-fragment angular distributions and the evaporation residue (ER) cross sections have been studied to understand the fusion-fission (FF) dynamics in the $^{32}S + ^{184}W$ reaction. Zhang *et al.* [18] have measured the

*prashant.patil0032@gmail.com

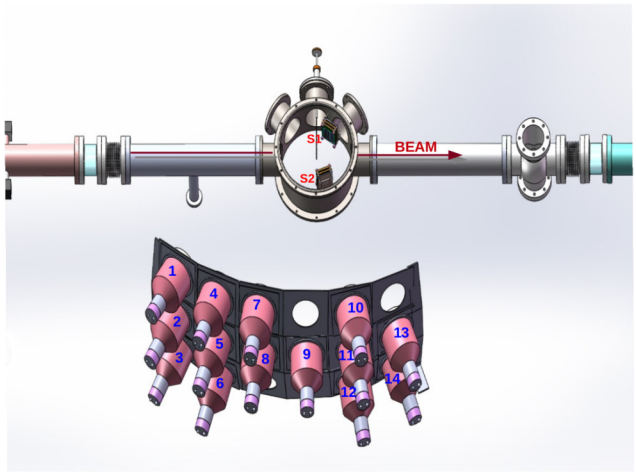

FIG. 1. Pictorial view of the of the experimental setup.

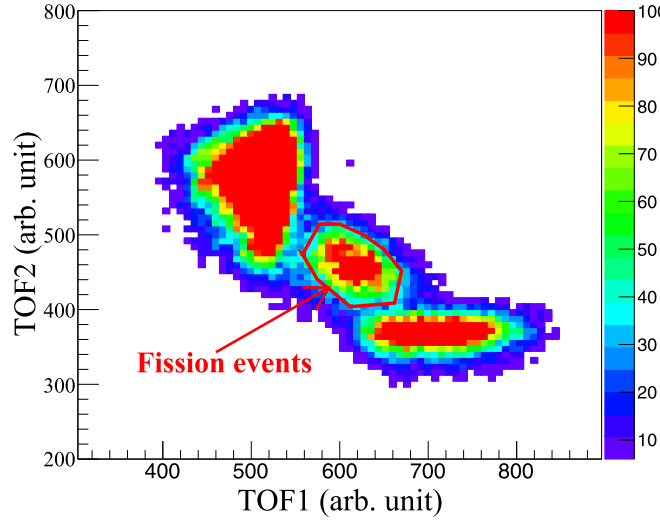

FIG. 2. Time of flight correlation plot obtained for S1 and S2 (see text).

fission fragments angular distributions for the $^{32}S + ^{184}W$ reaction and found comparable contributions from FF and quasifission (QF) fragments. Back *et al.* [19] have measured the ER cross sections for the $^{32}S + ^{184}W$ reaction and reported that the β depends strongly on the shell structure of the compound nuclear system. In the present work, we have investigated the fission dynamics in the formation and decay of the CN ^{216}Th populated in the fusion reaction of ^{32}S projectile on ^{184}W target at $E^* = 71.31$ MeV using pre-scission neutron multiplicity as a probe. Neutron energy spectra were measured at six different angles with respect to the fission fragment directions (6.8°, 14.2°, 21.8°, 38.8°, 54.8°, and 70.8°) and were analyzed to deduce pre-scission and post-scission neutron emission components.

This paper is organized as follows. The experimental procedure is described in Sec. II, accompanied by discussion on data analysis and obtained results in Sec. III. Section IV, provides the description of dynamical and statistical model analyses and confers a general discussion on the findings from the investigation. Finally, the results of the analyses were summarized and concluded in Sec. V.

II. EXPERIMENTAL PROCEDURE

The present experiment was carried out at the BARC-TIFR 14UD Pelletron-Linac accelerator facility, Mumbai. The pictorial view of the experimental setup is shown in Fig. 1. Pulsed beam of ^{32}S with 180 MeV beam energy ($E_{\rm beam}$) corresponding to an E^* of 71.31 MeV with a pulse separation of 107 ns was bombarded on the self-supported ^{184}W target of thickness 300 μg cm^{-2} to populate the CN ^{216}Th. Two 5 cm × 5 cm single-sided silicon strip detectors (S1, S2) were used to detect the complimentary fission fragments simultaneously. Each of these detectors have 16 strips and were placed at a distance of 10 cm and 12.6 cm away from the target on movable arms on either sides of the beam axis at angles of 64.5° (S1) and 72.5° (S2), respectively, inside a thin-walled scattering chamber of 32 cm diameter and 3 mm thickness.

Time of flight (TOF) of the fission fragments with reference to the onset of the beam were obtained from timing signals from S1 and S2 detectors, from which it is possible to isolate the fission events from projectile and targetlike events. Two-dimensional TOF spectra thus obtained from S1 and S2 is shown in Fig. 2. The timing correlation events corresponding to the fission-fragments is encircled by red line and also marked by an arrow. Also an energy gate on S1 and S2 has been applied to clearly separate projectile and targetlike events from the fission events.

An array of 14 liquid scintillators (5 inch dia and 2 inch thick cylindrical) situated at a distance of 72 cm from the target were used to record the neutrons in coincidence with the binary fission fragments [20]. These detectors are arranged in such a way to give different neutron angles with respect to one of the fission fragments as shown in Table I (angular separation ≈±16°).

The TOF signals were calibrated using precision time calibrator. TOF for neutron was obtained with reference to the time of flight of γ and converted into neutron energy spectrum on an event-by-event basis. A gate as shown in Fig. 2 is used to identify fission events and to generate the neutron energy spectra. The beam dump was placed at 3 m downstream from the target and the beam line was well shielded with layers of lead bricks and borated paraffin to block the scattered neutrons from reaching neutron detector. The neutron was discriminated from γ ray by generating a two-dimensional correlation plot of pulse shape discrimination (PSD) versus TOF as shown in Fig. 3. The energy-dependent efficiencies of the liquid scintillator detectors were obtained from

TABLE I. Neutron detector angles (θ) with respect to beam direction.

Detector No.	13, 14	10, 11, 12	9	7, 8	4, 5, 6	1, 2, 3
θ	58.3°	79.3°	95.3°	111.3°	127.3°	143.3°

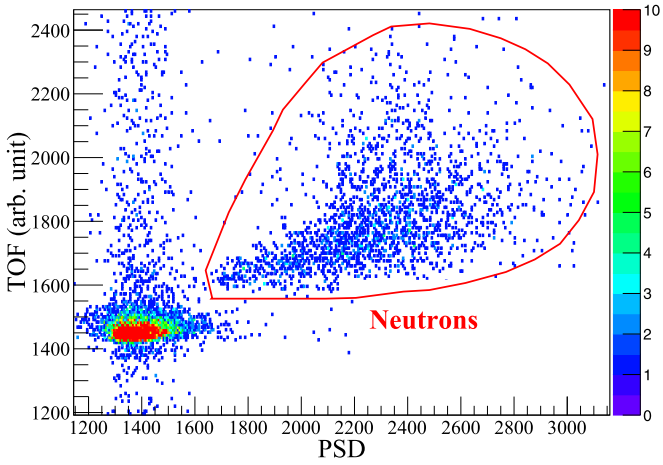

FIG. 3. Pulse shape discrimination (PSD) versus time-of-flight spectra (TOF) of one of the neutron detectors.

fission fragment-neutron coincident measurements using a ^{252}Cf source. The obtained efficiencies were then compared with the Monte Carlo simulations [21,22], which yielded results well in agreement with the experimental measurements. The energy detection threshold of 121 keV is obtained by calibrating the energy deposited in the scintillators with ^{137}Cs and ^{60}Co γ sources. The filtered RF (logical OR of the two fission fragments AND-gated with RF of the pulsed beam) was used as the trigger of the data acquisition system. A VME-based data acquisition using LAMPS software was used to acquire data in list mode.

III. DATA ANALYSIS AND RESULTS

In the present analysis any one of the triggered signals from S1, S2 detectors filtered with RF formed the master strobe for the data acquisition system. Now with respect to the filtered RF signal all the neutron TOF signals have been recorded. The measured neutron TOF spectra were converted into neutron energy spectra using following relations:

$$E_k = (\gamma - 1) \times M_n \times c^2 \tag{1}$$

$$\gamma = \frac{1}{\left(1 - \beta_n^2\right)^{1/2}} \tag{2}$$

$$\beta_n = \frac{v_n}{c} \tag{3}$$

$$v_n = \frac{D}{t_n}, \tag{4}$$

where the terms E_k, M_n, and v_n represent energy, mass, and velocity of neutrons. The term t_n represents time taken by emitted neutrons to reach the neutron detector. D is the flight path between the target and neutron detector. In order to obtain the pre- and post-scission neutron components, the observed neutron energy spectra were fitted with three moving-source evaporation components (the pre-scission component corresponding to emission from composite nucleus and the post-scission components corresponding to emission from the two fission fragments) using the Watt expression [9,23]:

$$\frac{d^2M}{dE_n d\Omega_n} = \sum_{i=1}^{3} \left\{ \frac{\nu_i {E_n}^{1/2}}{2(\pi T_i)^{3/2}} \right\} \times \exp\left\{ - \frac{E_n - 2(E_n E_i/A_i)^{1/2} \cos\theta_i + E_i/A_i}{T_i} \right\} \tag{5}$$

where E_n is the measured neutron energy in the laboratory frame, ν_i, A_i, E_i, and T_i are multiplicity, mass, kinetic energy, and temperature, respectively, of each neutron emitter. θ_i is the relative angle between the emitted neutron with respect to its source. Assuming symmetric fission of CN the kinetic energy of the fission fragments was calculated from Viola systematics [24].

In the present analysis simultaneous fitting has been carried out for neutron energy spectra in the energy range 2–6 MeV at different angles on event-by-event basis after taking into account the relative angle between neutron and one of the fission fragments using 14 liquid scintillator neutron detector array. The simultaneous fitting has been done in two approaches. In the first approach, pre-scission neutron multiplicity ($\nu_{\rm pre}$), post-scission neutron multiplicity ($\nu_{\rm post}$), and their corresponding temperatures ($T_{\rm pre}$, $T_{\rm post}$) were treated as free parameters. The simultaneous fitting is also done by fixing the value of $T_{\rm pre}$ according to the formula $T_{\rm pre} = \sqrt{\frac{E^*}{a}}$, where E^* is the excitation energy and a is the nuclear level density parameter, taken as $a = \frac{A_{CN}}{10}$ MeV^{-1}. The $\nu_{\rm pre}$ values obtained from fixed $T_{\rm pre}$ are comparable with those obtained from treating $T_{\rm pre}$ as a free parameter. Total neutron multiplicity ($\nu_{\rm tot}$) is then obtained from the equation: $\nu_{\rm tot} = \nu_{\rm pre} + 2 \times \nu_{\rm post}$. A typical simultaneous fitted plot of double differential neutron multiplicity spectra for ^{32}S + ^{184}W reaction at $E^* = 71.31$ MeV for various correlation angles with respect to fission fragments is shown in Fig. 4 and the best fit values of $\nu_{\rm pre}$, $\nu_{\rm post}$, $\nu_{\rm tot}$, $T_{\rm pre}$, and $T_{\rm post}$ were summarized in Table II.

From the deduced pre- and post-scission multiplicities an amount of initial excitation energy remained in the system at scission point can be determined. Based on Hilscher and Rossner systematics of spontaneous and neutron-induced fission, an average of 2.9 neutrons were emitted in the low-energy fission of Th nucleus [25]. Total excitation energy (E^*_{av}) available for fission can be estimated from the following equation:

$$E^*_{av} = E^* + Q_F - \langle TKE \rangle, \tag{6}$$

where E^* is the excitation energy of the compound nucleus, Q_F is the Q value for compound nucleus fission and $\langle TKE \rangle$ is the total kinetic energy of the fission fragments. The value of Q_F is given by $Q_F = M_{CN}$-M_{F1}-M_{F2}, where M_{F1} and M_{F2} are the masses of two fragments [26]. From Eq. (6), E^*_{av} available for fission was estimated to be $\simeq$83.86 MeV. The overall neutron cost also includes the emission of γ rays, which carry an energy of 10 MeV along the deexcitation cascade [27]. Consequently, from deduced post-scission multiplicity it was found that an initial excitation energy of $\simeq$40.75 MeV was not removed by neutron emission before scission, which in

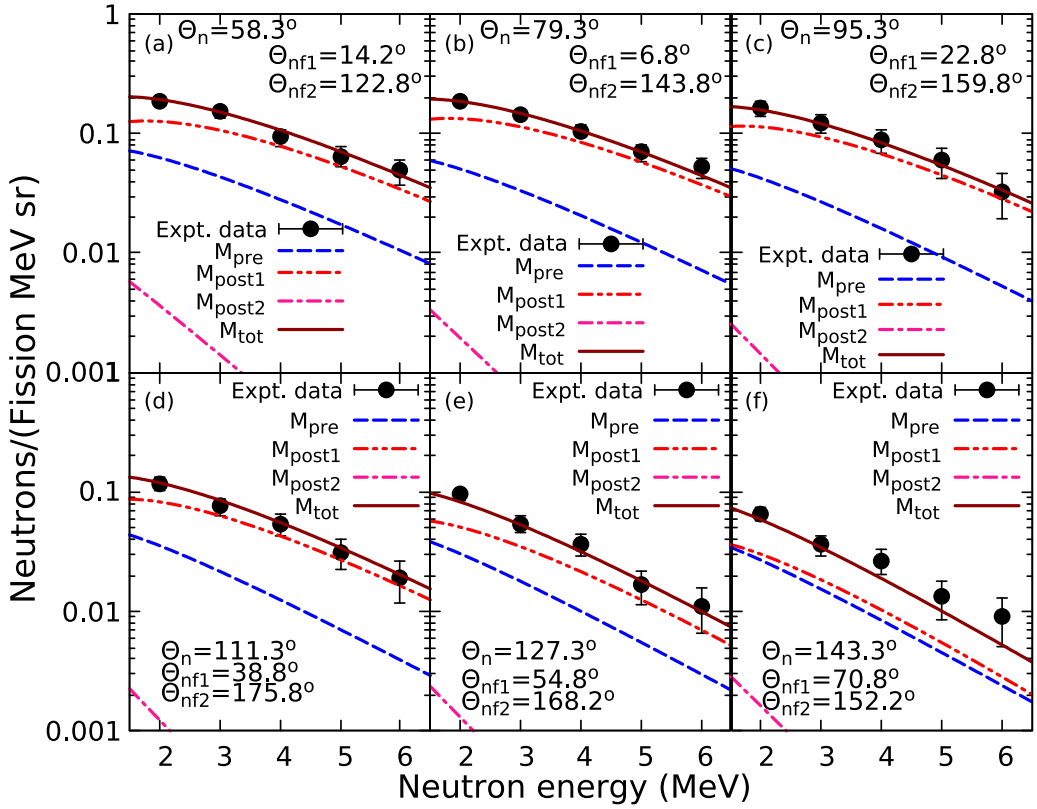

FIG. 4. Experimental double differential neutron multiplicity spectra (solid circles) from ^{216}Th CN at an excitation energy of 71.3 MeV for 14 neutron detectors in/out of the reaction plane. The multiple moving source fits for the pre-scission (blue dashed lines) and post-scission contribution from one fragment (red double dotted lines) and that from the other (dark-pink single dotted lines) are also shown. The total contribution from all the three sources are indicated by the dark-red line.

turn indicates that the energy cost for emission of neutrons is of 12.35 MeV and the average number of neutrons evaporated per MeV is 0.08. The effective Q value ($Q_{\rm eff}$) for the fission can be estimated from the following equation:

$$Q_{\rm eff} = Q_F - \langle TKE \rangle. \tag{7}$$

Thus a value of $Q_{\rm eff} \simeq 12.55$ MeV was expected to be remained at scission point. But from the measured post-scission neutron multiplicity it was found that the substantial amount of initial excitation energy $\simeq 40.75$ MeV was not removed by neutron emission prior to scission. Similar analysis for ^{16}O + ^{208}Pb reaction at an $E^* \simeq 72.56$ MeV has shown a value of $Q_{\rm eff} \simeq 13.57$ MeV and further indicated that an initial excitation energy of $\simeq$38.53 MeV was not removed by neutron emission before scission. These analyses suggest that fissioning nucleus of ^{32}S + ^{184}W reaction has relatively higher elongation compared to ^{16}O + ^{208}Pb reaction.

IV. DISCUSSION

A. Dynamical model calculations

In the present work dynamical model HICOL code calculations developed by Feldmier [28] have been carried out to estimate the formation time for the reaction under study and for the ^{16}O + ^{208}Pb reaction leading to the CN ^{224}Th. The dynamical model treats colliding nuclei as two spheres of Fermi gas and allows exchange of particles, momentum, and entropy through a window in the mean single-particle potential. Time progression in the colliding trajectories are estimated by solving a Langevin equation with fluctuating dissipative force. The behavior of fluctuating force is understood in terms of microscopic picture of particle exchange between two nuclei. The model assumes two spheres are connected by a neck and their dynamical evolution described by a sequence of shapes; and the mass and charged density remain constant during the collision to conserve the volume of shape. The macroscopic shapes of the nuclear system are represented

TABLE II. Experimentally obtained $\nu_{\rm pre}$, $\nu_{\rm post}$, $\nu_{\rm tot}$, $T_{\rm pre}$, and $T_{\rm post}$ values.

E^* (MeV)	$\nu_{\rm pre}$	$\nu_{\rm post}$	$\nu_{\rm tot}$	$T_{\rm pre}$	$T_{\rm post}$
71.3	2.68 ± 0.48	3.30 ± 0.20	5.98 ± 0.56	1.55 ± 0.35	1.16 ± 0.10

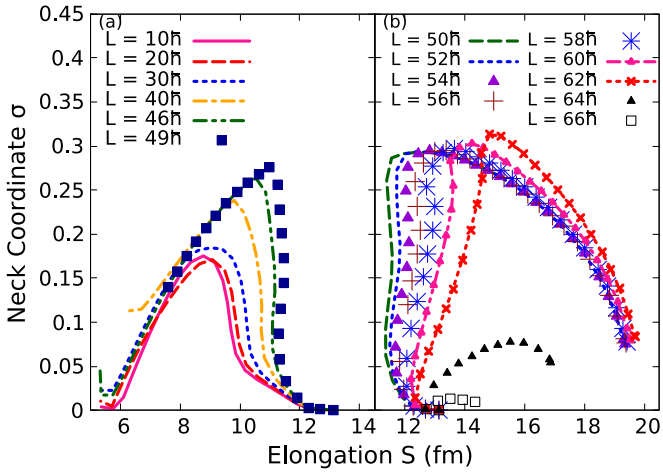

FIG. 5. Neck coordinate versus elongation for fusion and nonfusion trajectories are shown in (a) and (b), respectively, in case $^{32}S + ^{184}W$ reaction.

by axially symmetric configurations with sharp surfaces. The shapes of evolving nuclei are uniquely determined by three macroscopic variables: the distance between the nuclei S, the neck coordinate σ, and the mass asymmetry Δ, which are defined as:

$$S = \text{distance between two sphere centers}$$

$$\sigma = \frac{V_o - (4\pi/3)R_1^3 - (4\pi/3)R_2^3}{V_o} \tag{8}$$

$$\Delta = \frac{R_1 - R_2}{R_1 + R_2}, \tag{9}$$

where V_o is the total volume of the system considered as independent of s, σ, Δ. R_1, R_2 are the radii of the two interacting nuclei.

The HICOL code included three more rotational degrees of freedom (intrinsic and relative) of the dinuclear complex in addition to three shape degrees of freedom. With the help of these shape and rotational coordinates, their evolution is traced by solving Langevin equations of motion. The system motion is strongly monitored from a strong dissipative force, which in turn depend on the friction and diffusion terms obtained from the particle exchange model as described in the work of Feldmeier [28]. One-body dissipation is assumed to be the dominant mechanism. In earlier work of Saxena *et al.* [27], the HICOL model has been successfully used to describe the fissionlike reactions in $^{28}Si + ^{232}Th$ system at 340 MeV and also to predict the reaction time scales required to describe available data on pre-scission neutron multiplicity. More recently HICOL predictions have shown consistency with experimental $\langle TKE \rangle$ values in the symmetric mass split for the reaction $^{50}Ti + ^{208}Pb$ at 294 MeV bombarding energy [29].

Figure 5 show typical fusion and nonfusion trajectories in the (S, σ) plane for selected angular momentum values for the $^{32}S + ^{184}W$ reaction. When distance between two sphere centers are about 13 fm apart, the trajectories start at $t = 0$. It is observed that the trajectories for $\ell = 10\hbar$, $20\hbar$, $30\hbar$, $40\hbar$, $42\hbar$, $44\hbar$, $46\hbar$, and $49\hbar$ correspond to typical fusion kind for which calculated trajectories would be ended when the minimum elongation is reached [29]. The case of $\ell = 50\hbar$, $\ell = 52\hbar$, $54\hbar$, $56\hbar$, and $58\hbar$ correspond to nonfusing trajectories for which the composite system develops a fat neck and reseparates into two nearly symmetric fragments without reaching the fusion condition. The mass asymmetry increases for nonfusing trajectories as a function of ℓ and at the higher angular momenta of $\ell = 60\hbar$ and $\ell = 62\hbar$ the system does not fully equilibrate in the mass degree of freedom and reseparates as projectile- and targetlike fragments. The trajectories, $\ell = 64\hbar$ and $\ell = 66\hbar$ correspond to quasielastic trajectories showing very little mass exchange.

Thus, dynamical HICOL model predictions show that trajectories corresponding to angular momentum values $\ell = (50 - 58)\hbar$ will lead to quasifission/fast-fission events and trajectories below $\ell = 50\hbar$ will lead to the compound nucleus formation. For the present system, HICOL code predicts around $\simeq$80% compound nucleus decay contribution and remaining $\simeq$20% by quasifission/fast-fission process. Similar results has been predicted by DNS model, where quasifission contribution is around $\simeq$28%, fast-fission contribution is around $\simeq$4% and remaining contribution is attributed to compound nucleus decay [31].

From fusion trajectories it is possible to estimate the τ_{fr} using the equation: $\int_{\ell=0}^{\ell=49} \frac{\sigma(\ell)\times T(\ell)}{\sigma(\ell)} d\ell$. Where $\sigma(\ell)$ is corresponds to partial fusion cross section obtained from CCFULL code [30] by fitting the measured captured cross section for the $^{32}S + ^{184}W$ reaction [31] and $T(\ell)$ is the formation time corresponding to each fusion trajectory (ℓ). A value of $\tau_{fr} = 19 \times 10^{-21}$ s has been obtained for the present system. By carrying out similar analysis for the $^{16}O + ^{208}Pb$ system forming ^{224}Th CN, $\simeq$89% contribution from the compound nucleus decay and $\simeq$ 11% contribution from quasifission/fast-fission process have been observed and $\tau_{fr} = 9 \times 10^{-21}$ s has been found. These analyses have been shown a higher value of τ_{fr} ($\tau_{fr} = 19 \times 10^{-21}$ s) for the $^{32}S + ^{184}W$ system in comparison to the $^{16}O + ^{208}Pb$ system ($\tau_{fr} = 9 \times 10^{-21}$ s).

B. Statistical model calculations

In order to understand the measured ν_{pre}, statistical model calculations have been carried out by incorporating the fission delay in JOANNE2 code [14]. JOANNE2 code accounts the pre-scission emission from two points in the deformation space, corresponding to mean presaddle deformation (Z_{tr}) and mean saddle-to-scission deformation (Z_{ssc}), (Z represents the symmetry axis elongation in units of the diameter of the corresponding spherical nucleus). The level density parameter a_n, corresponding to spherical CN and deformation-dependent level densities (a_{ssc}) corresponding to each Z_{ssc} were incorporated from the prescription of Toke and Swiatecki [32]. The effects of deformation dependence of particle-binding energies and particle transmission coefficients on fission time scales were taken from Refs. [14,33]. The rotating finite-range model (RFRM) fission barrier is used in the code without any scaling for the determination of fission barrier height [34].

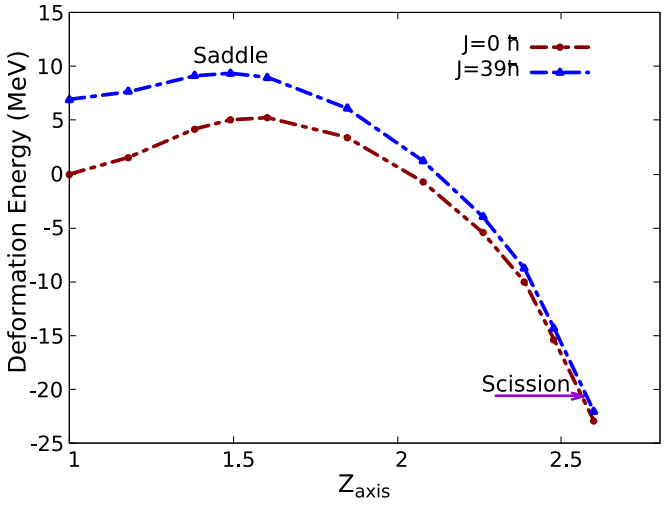

FIG. 6. The potential energy diagram for ^{216}Th showing deformation energy as a function of elongation Z_{axis} for angular momentum $J = 0\ \hbar$ and $J = 39\ \hbar$ (average of compound nucleus angular distribution).

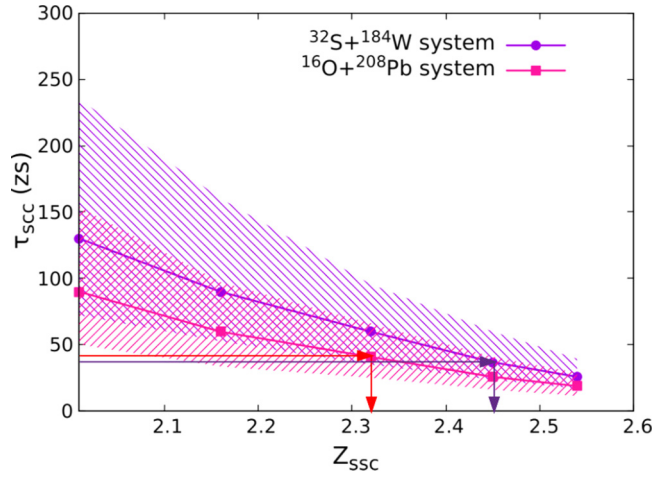

FIG. 8. The variation of τ_{ssc} as a function of Z_{ssc}. Here 1 zs = 10^{-21} s. The shaded region corresponds to the values of τ_{ssc} required to reproduce experimental errors of ν_{pre}.

Fusion cross sections were calculated using the CCFULL code [30].

In the present work presaddle time (τ_{tr}) $\simeq 10 \times 10^{-21}$ s has been obtained using JOANNE2 code by reproducing the evaporation cross sections of above reaction at an $E^* \simeq$ 71.31 MeV [19]. Figure 6 shows the potential energy diagram in terms of the simplified rotating liquid drop model incorporated in JOANNE2 code for the reaction under study. The Z_{ssc} was varied between 1.8–2.57. Figure 7 shows the variation of binding energies with deformation for CN ^{216}Th. It can be seen that particle binding energy increases with Z_{axis} for proton and α emission and where as for neutron it decreases. The statistical model code JOANNE2 predicts ν_{pre} of 0.62 without any fission delay. The excess $\nu_{\text{pre}} = 2.06 \pm 0.48$ in comparison to statistical model JOANNE2 code prediction were converted into total fission delay (τ_{tot}). The mean evaporation lifetime for the present reaction for various neutrons emission has been estimated from statistical model code PACE4 [35,36]. The τ_{tot} is obtained by summing the time delays involved in the emission of the observed excess neutrons [9]. The value for τ_{tot} as deduced from this analysis is found to be about $66^{+20}_{-20} \times 10^{-21}$ s for the present ^{32}S + ^{184}W reaction for the level density parameter $a = A_{CN}/10.0\ \text{MeV}^{-1}$ and $a_n/a_s = 1.0$ (a_n and a_s are the level density parameters for the spherical CN and at the saddle point, respectively). The saddle to scission delay (τ_{ssc}) of $37^{+20}_{-20} \times 10^{-21}$ s has been obtained by subtracting the τ_{tr} and τ_{fr} from τ_{tot}. A comparative study of fission delay has been carried out for the ^{16}O + ^{208}Pb reaction leading to CN ^{224}Th. From literature $\nu_{\text{pre}} = 3.4 \pm 0.5$ has been observed for the ^{16}O + ^{208}Pb reaction at an $E^* \simeq$ 72.56 MeV [37]. The code JOANNE2 predicts ν_{pre} of 1.13 without any fission delay. The excess $\nu_{\text{pre}} = 2.27 \pm 0.5$ in comparison to JOANNE2 code prediction were converted into τ_{tot} of $60^{+23}_{-23} \times 10^{-21}$ s. A similar value of $\tau_{tr} \simeq 10 \times 10^{-21}$ s has been used and $\tau_{fr} \simeq 9 \times 10^{-21}$ s has been estimated using HICOL code prediction. Consequently, $\tau_{ssc} = 41^{+23}_{-23} \times 10^{-21}$ s has been obtained in case ^{16}O + ^{208}Pb reaction.

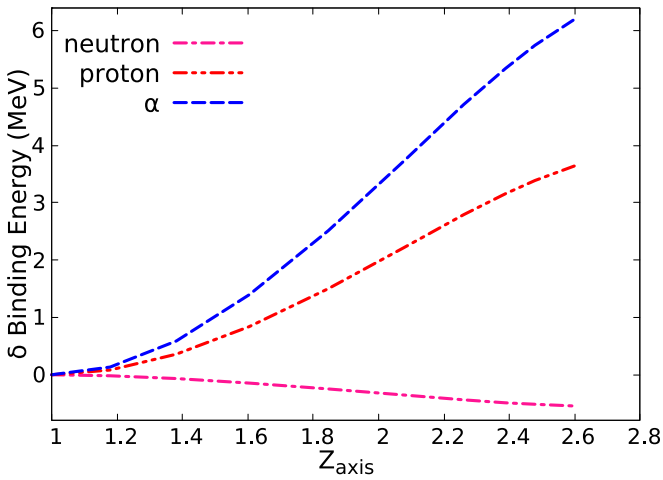

FIG. 7. Deformed liquid drop model predictions of the deviation of binding energies from spherical nucleus for neutron, proton, and α particle emission for ^{32}S + ^{184}W system.

From Fig. 8 it has been observed that for the measured pre-scission multiplicities of ^{32}S + ^{184}W and ^{16}O + ^{208}Pb systems, the τ_{ssc} values depend on values of the Z_{ssc}. The values of τ_{ssc} ($\tau_{ssc} \simeq 37 \times 10^{-21}$ s for ^{32}S + ^{184}W system and $\tau_{ssc} \simeq 41 \times 10^{-21}$ s for ^{16}O + ^{208}Pb system) and Z_{ssc} ($Z_{ssc} = 2.45$ for ^{32}S + ^{184}W system and $Z_{ssc} = 2.32$ for ^{16}O + ^{208}Pb system) for above two systems have been indicated by indigo and red color arrows, respectively. Statistical model calculations have also been performed for fixed τ_{tr} and Z_{ssc} to reproduce measured ν_{pre} and calculated τ_{ssc} of above two systems within error regions. It is seen from Fig. 9 that $\nu_{\text{pre}} = 2.68 \pm 0.48$ and $\tau_{ssc} = 37^{+20}_{-20} \times 10^{-21}$ s of ^{32}S + ^{184}W system and $\nu_{\text{pre}} = 3.40 \pm 0.50$ and $\tau_{ssc} = 41^{+23}_{-23} \times 10^{-21}$ s of ^{16}O + ^{208}Pb system were substantially

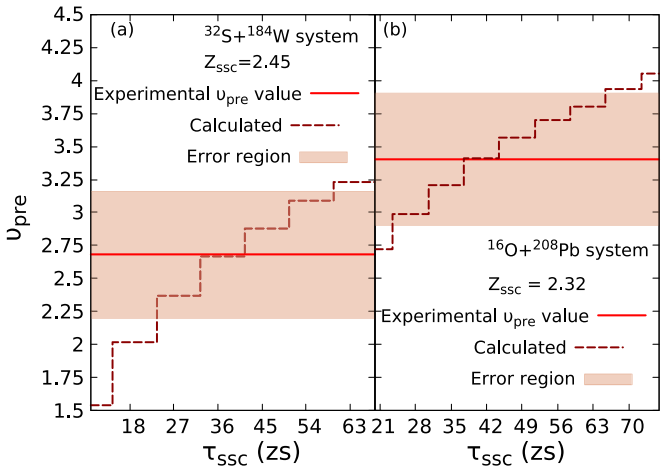

FIG. 9. The variation of $\nu_{\rm pre}$ as a function of τ_{ssc} for ^{32}S + ^{184}W system in (a) and for ^{16}O + ^{208}Pb system in (b). Here 1 zs = 10^{-21} s. The shaded region corresponds to experimental errors of $\nu_{\rm pre}$.

reproduced by $Z_{ssc} = 2.45$ and $Z_{ssc} = 2.32$, respectively. The experimentally measured $\nu_{\rm pre}$ values of above systems were shown as red lines within the shaded error regions.

The difference of Z_{ssc} observed in the above two reactions can be understood in terms of elongated fission configuration of ^{32}S + ^{184}W system in comparison to relatively compact fission configuration of ^{16}O + ^{208}Pb system. ^{16}O projectile and ^{208}Pb target are spherical in nature where ^{32}S projectile and ^{184}W are prolate deformed [38]. The observed Z_{ssc} for ^{32}S + ^{184}W system is consistent with measured neutron multiplicities from which it has been observed that a substantial amount of initial excitation energy remains at scission point indicating elongated configuration for fissioning nucleus. A slightly lower value of τ_{ssc} for ^{32}S + ^{184}W system in comparison to ^{16}O + ^{208}Pb system can be understood by higher quasifission percentage prediction by HICOL code for former system in comparison to latter system. These observations suggest that observed fission delay for ^{32}S + ^{184}W system and ^{16}O + ^{208}Pb system can be understood quantitatively if we considered different τ_{fr} values as predicted by dynamical code HICOL.

V. SUMMARY AND CONCLUSIONS

The present work describes the fragment-fragment-neutron correlation measurement in the collisions of ^{32}S projectile on ^{184}W target at 180 MeV bombarding energy. Pre-scission neutron multiplicity = 2.68 ± 0.48 and post-scission neutron multiplicity = 3.3 ± 0.20 have been deduced from multi-source fits to the observed neutron energy spectra. Dynamical model HICOL code predictions have shown $\tau_{fr} \simeq 19 \times 10^{-21}$ s for the present system and $\tau_{fr} \simeq 9 \times 10^{-21}$ s for the ^{16}O + ^{208}Pb system. The HICOL code analyses have predicted a higher value of τ_{fr} for the present symmetric system in comparison to the asymmetric ^{16}O + ^{208}Pb system for the case where both systems are lying lower side of α_{BG}.

For the ^{32}S + ^{184}W reaction we have simultaneously reproduced both measured $\nu_{\rm pre}$ and available ER cross section at an E^* ≃71.31 MeV within the framework of statistical model JOANNE2 code by considering fission delay, deformation-dependent particle binding energies, charged particle transmission coefficients, and level densities. The excess $\nu_{\rm pre} = 2.06 \pm 0.48$ were converted into $\tau_{\rm tot}$ of $66^{+20}_{-20} \times 10^{-21}$ s. The JOANNE2 code analyses have shown that the $\tau_{tr} = 10 \times 10^{-21}$ s is required to account the ER cross section and $\tau_{ssc} = 37^{+20}_{-20} \times 10^{-21}$ s is required to account the excess $\nu_{\rm pre}$ for the present system. A comparative study of fission delay for the ^{16}O + ^{208}Pb system has shown $\tau_{\rm tot} = 60^{+23}_{-23} \times 10^{-21}$ s and $\tau_{ssc} = 41^{+23}_{-23} \times 10^{-21}$ s for the excess $\nu_{\rm pre} = 2.27 \pm 0.50$. A slightly lower value of τ_{ssc} for ^{32}S + ^{184}W system in comparison to ^{16}O + ^{208}Pb system can be understood by higher quasifission percentage prediction by HICOL code for former system in comparison to latter system. These analyses illustrate that fission delay for both systems can be understood by considering different τ_{fr} values as predicted by HICOL code.

The JOANNE2 code analysis has shown, $Z_{ssc} = 2.45$ is required to account the observed τ_{ssc} and $\nu_{\rm pre}$ for the present reaction and $Z_{ssc} = 2.32$ is required for ^{16}O + ^{208}Pb reaction. The difference of Z_{ssc} observed in the above two reactions can be understood in terms of elongated fission configuration of ^{32}S + ^{184}W system in comparison to relatively compact fission configuration of ^{16}O + ^{208}Pb system.

ACKNOWLEDGMENTS

One of the authors (N.M.B.) would like to thank IUAC-UGC, Government of India for sanction of the research project (Sanction No. IUAC/XIII.7/UFR-60310) as well as financial support through fellowship to the author (P.N.P.). The authors are thankful to Dr. A. Chatterjee for providing the moving source fit code. The help from the Pelletron accelerator staff for smooth running of the accelerator during the experiment is gratefully acknowledged.

[1] R. Mahajan, B. R. Behera, M. Thakur, G. Kaur, P. Sharma, K. Kapoor *et al.*, Phys. Rev. C **98**, 034601 (2018).
[2] M. Thakur, B. R. Behera, R. Mahajan, G. Kaur, P. Sharma, K. Kapoor *et al.*, Phys. Rev. C **98**, 014606 (2018).
[3] M. Shareef, E. Prasad, A. Jhingan, N. Saneesh, K. S. Golda, A. M. Vinodkumar *et al.*, Phys. Rev. C **99**, 024618 (2019).
[4] N. K. Rai, A. Gandhi, Ajay Kumar, N. Saneesh, M. Kumar, G. Kaur *et al.*, Phys. Rev. C **100**, 014614 (2019).
[5] K. S. Golda *et al.*, Nucl. Phys. A **913**, 157 (2013).
[6] A. Pal, S. Santra, D. Chattopadhyay, A. Kundu, A. Jhingan, P. Sugathan *et al.*, Phys. Rev. C **98**, 031601(R) (2018).
[7] G. Mohanto *et al.*, Phys. Rev. C **97**, 054603 (2018).
[8] H. Singh *et al.*, Phys. Rev. C **78**, 024609 (2008).
[9] A. Saxena, A. Chatterjee, R. K. Choudhury, and S. S. Kapoor, and D. M. Nadkarni, Phys. Rev. C **49**, 932 (1994).
[10] Y. Wei, Chin. Phys. Lett. **20**, 482 (2003).

[11] R. Sandal, B. R. Behera, V. Singh, M. Kaur, A. Kumar, G. Singh *et al.*, Phys. Rev. C **87**, 014604 (2013).
[12] Y. K. Gupta *et al.*, Phys. Rev. C **84**, 031603(R) (2011).
[13] K. Kapoor, S. Verma, P. Sharma, R. Mahajan, N. Kaur, G. Kaur *et al.*, Phys. Rev. C **96**, 054605 (2017).
[14] J. P. Lestone, Phys. Rev. Lett. **70**, 2245 (1993).
[15] D. J. Hinde, H. Ogata, M. Tanaka, T. Shimoda, N. Takahashi, A. Shinohara, S. Wakamatsu, K. Katori, and H. Okamura, Phys. Rev. C **39**, 2268 (1989).
[16] K. Ramachandran *et al.*, Phys. Rev. C **73**, 064609 (2006).
[17] H. A. Kramers, Physica **7**, 284 (1940).
[18] H. Q. Zhang *et al.*, Nucl. Phys. A **834**, 201c (2010).
[19] B. B. Back, D. J. Blumenthal, C. N. Davids, D. J. Henderson, R. Hermann, D. J. Hofman, C. L. Jiang, H. T. Penttila, and A. H. Wuosmaa, Phys. Rev. C **60**, 044602 (1999).
[20] P. C. Rout *et al.*, JINST **13**, P01027 (2018).
[21] W. Mannhart, in *Proceedings of IAEA Advisory Group Meeting, Properties of Neutron Sources, TECDOC-410* (International Atomic Energy Agency, Vienna, 1987), p. 158.
[22] W. Mannhart, INDC(NDS)-210, 305 (International Atomic Energy Agency, Vienna, 1989), pp. 305–336.
[23] E. Holub, D. Hilscher, G. Ingold, U. Jahnke, H. Orf, and H. Rossner, Phys. Rev. C **28**, 252 (1983).
[24] V. E. Viola, K. Kwiatkowski, and M. Walker, Phys. Rev. C **31**, 1550 (1985).
[25] D. Hilscher and H. Rossner, Ann. Phys. Fr. **17**, 471 (1992).
[26] R. G. Thomas, A. Saxena, P. K. Sahu, R. K. Choudhury, I. M. Govil, S. Kailas *et al.*, Phys. Rev. C **75**, 024604 (2007).
[27] A. Saxena, D. Fabris, G. Prete, D. V. Shetty, G. Viesti, B. K. Nayak *et al.*, Nucl. Phys. A **730**, 299 (2004).
[28] H. Feldmeier, Rep. Prog. Phys. **50**, 915 (1987).
[29] S. Appannababu, M. Cinausero, T. Marchi, F. Gramegna, G. Prete, J. Bermudez *et al.*, Phys. Rev. C **94**, 044618 (2016).
[30] Hagino *et al.*, Comput. Phys. Commun. **123**, 143 (1999).
[31] H. Q. Zhang, C. L. Zhang, C. J. Lin, Z. H. Liu, F. Yang, A. K. Nasirov, G. Mandaglio, M. Manganaro, and G. Giardina, Phys. Rev. C **81**, 034611 (2010).
[32] J. Toke and W. J. Swiatecki, Nucl. Phys. A **372**, 141 (1981).
[33] J. P. Lestone *et al.*, Nucl. Phys. A **559**, 277 (1993).
[34] A. J. Sierk, Phys. Rev. C **33**, 2039 (1986).
[35] O. B. Tarasov and D. Bazin, Nucl. Instrum. Methods Phys. Res., Sect. B **204**, 174 (2003).
[36] O. B. Tarasov and D. Bazin, Nucl. Instrum. Methods Phys. Res., Sect. B **266**, 4657 (2008).
[37] H. Rossner, D. J. Hinde, J. R. Leigh, J. P. Lestone, J. O. Newton, J. X. Wei, and S. Elfstrom, Phys. Rev. C **45**, 719 (1992).
[38] P. Moller, A. J. Sierk, T. Ichikawa, and H. Sagawa, At. Data Nucl. Data Tables, **109–110**, 1 (2016).